HIGHLY METHYL ESTERIFIED SEEDS Is a Pectin Methyl Esterase Involved in Embryo Development[1][OPEN]

Gabriel Levesque-Tremblay, Kerstin Müller, Shawn D. Mansfield, and George W. Haughn*

Departments of Botany (G.L.-T., G.W.H.) and Wood Science (S.D.M.), Faculty of Forestry, University of British Columbia, Vancouver, British Columbia, Canada V6T 1Z4; and Department of Biological Science, Simon Fraser University, Burnaby, British Columbia, Canada V5A 1S6 (K.M.)

Homogalacturonan pectin domains are synthesized in a highly methyl-esterified form that later can be differentially demethyl esterified by pectin methyl esterase (PME) to strengthen or loosen plant cell walls that contain pectin, including seed coat mucilage, a specialized secondary cell wall of seed coat epidermal cells. As a means to identify the active PMEs in seed coat mucilage, we identified seven PMEs expressed during seed coat development. One of these, *HIGHLY METHYL ESTERIFIED SEEDS* (*HMS*), is abundant during mucilage secretion, peaking at 7 d postanthesis in both the seed coat and the embryo. We have determined that this gene is required for normal levels of PME activity and homogalacturonan methyl esterification in the seed. The *hms-1* mutant displays altered embryo morphology and mucilage extrusion, both of which are a consequence of defects in embryo development. A significant decrease in the size of cells in the embryo suggests that the changes in embryo morphology are a consequence of lack of cell expansion. Progeny from a cross between *hms-1* and the previously characterized *PME inhibitor5 overexpression line* suggest that HMS acts independently from other cell wall-modifying enzymes in the embryo. We propose that HMS is required for cell wall loosening in the embryo to facilitate cell expansion during the accumulation of storage reserves and that its role in the seed coat is masked by redundancy.

Plant cell walls are complex composites composed of a variety of polysaccharides, proteins, and aromatic or aliphatic compounds (Caffall and Mohnen, 2009). Pectins are acidic heteropolymers that form a hydrated gel, in which cellulose and other molecules are embedded in the plant cell wall. Increasing evidence supports the hypothesis that all three of the major pectin classes, homoglacturonan (HG), rhamnogalacturonan I, and rhamnogalacturonan II, are covalently linked in the cell wall (Willats et al., 2001; Caffall and Mohnen, 2009; Tan et al., 2013), forming a hydrophilic macromolecular network. The most abundant pectin is HG, a polymer of GalA (Ridley et al., 2001) thought to be synthesized in a highly methyl-esterified form that can be demethyl esterified after secretion to the apoplast (Zhang and Staehelin, 1992; Staehelin and Moore, 1995; Sterling et al., 2001). Demethyl esterification is catalyzed by pectin methyl esterases (PMEs) in either a blockwise or nonblockwise fashion (Wakabayashi et al., 2003). When a PME acts in a blockwise fashion, removing methyl groups from at least 10 consecutive adjacent GalA residues, the free carboxyl groups created can interact with Ca^{2+}, forming a pectic gel (Goldberg et al., 1996; Al-Qsous et al., 2004). In contrast, PME action may expose glycosidic bonds between adjacent GalA residues for subsequent polygalacturonase-mediated hydrolysis that would be expected to participate in cell wall loosening and extension (Moustacas et al., 1991). Pectin methyl esterase inhibitors (PMEIs) are small proteins that have been shown to inhibit PMEs, and these enzymes must also be taken into account when studying PME-related cell wall modification (Pelloux et al., 2007).

PMEs and PMEIs have been shown to be involved in diverse physiological processes (Micheli, 2001; Pelloux et al., 2007; Wolf et al., 2009; Jolie et al., 2010), including cell wall elongation and organogenesis (Peaucelle et al., 2008, 2011; Pelletier et al., 2010). Arabidopsis (*Arabidopsis thaliana*) PMEs and PMEIs are encoded by two large gene families consisting of 66 and 69 genes, respectively (http://www.cazy.org/), which seem to have expanded as a result of a duplication event and then evolved to have divergent spatiotemporal specialization (Wang et al., 2013).

The epidermal cell layer of Arabidopsis seed coat undergoes complex cell differentiation, during which large quantities of pectinaceous mucilage are secreted between the plasma membrane and the outer tangential primary cell wall (Haughn and Western, 2012; North et al., 2014). Upon exposure to water, mucilage is extruded from the epidermal cells and encapsulates the mature seed. Several lines of evidence indicate that HG, the substrate of PME, is present in seed coat mucilage. First, monosaccharide analysis of Arabidopsis seed coat mucilage suggests a

[1] This work was supported by the Natural Sciences and Engineering Research Council of Canada (Postgraduate Doctoral Scholarship to G.L.-T. and Discovery Grants to S.D.M. and G.W.H.) and the European Commission (Marie Curie International Outgoing Fellowship to K.M.).

* Address correspondence to george.haughn@ubc.ca.

The author responsible for distribution of materials integral to the findings presented in this article in accordance with the policy described in the Instructions for Authors (www.plantphysiol.org) is: George W. Haughn (george.haughn@ubc.ca).

[OPEN] Articles can be viewed without a subscription.

www.plantphysiol.org/cgi/doi/10.1104/pp.114.255604

small proportion of HG (Dean et al., 2007; Macquet et al., 2007). Second, plants homozygous for a mutation in a gene, *GALACTURONOSYLTRANSFERASE11*, encoding an HG biosynthetic enzyme, produce seeds with lower quantities of mucilage (Caffall et al., 2009). Third, seed mucilage is recognized by HG-specific antibodies John Innes Monoclonal Antibody5 (JIM5), JIM7, PAM1, and 2F4 (Willats et al., 2001; Macquet et al., 2007; Voiniciuc et al., 2013).

Evidence for the presence of PMEs and PMEIs in seed development is largely related to the identification of their transcripts in seed tissues. Approximately 20 PMEs are expressed during silique development (Louvet et al., 2006), whereas real-time PCR data and promoter-GUS fusions have shown that two PME genes are expressed early in seed development (Louvet et al., 2006). Another study identified genes annotated to encode PME and PMEI proteins specifically expressed in the seed coat, endosperm, or embryo during development (Wolf et al., 2009). Recently, FLYING SAUCER1 (FLY1), a transmembrane ring E3 Ubiquitin Ligase, was shown to regulate the degree of pectin methyl esterification in Arabidopsis seed mucilage (Voiniciuc et al., 2013), highlighting the importance of PME and its inhibitors in the seed coat. Voiniciuc et al. (2013) proposed that FLY1 regulates the degree of pectin methyl esterification in mucilage by recycling PME enzymes from the apoplast of seed coat epidermal cells. SUBTILISIN-LIKE SER PROTEASE1 (SBT1) was shown to be a protease essential for normal seed mucilage release (Rautengarten et al., 2008). The mutant *atsbt1.7* has increased PME activity in the seeds, suggesting that it acts as a repressor of PME activity. Most recently, PMEI6 was shown to promote Arabidopsis seed mucilage release by limiting methyl esterification of homogalacturonan in seed coat epidermal cells (Saez-Aguayo et al., 2013). Given that PMEIs are believed to function with PMEs, these data indirectly support the importance of PME activity in seed mucilage biosynthesis.

Here, we sought to identify the PMEs that function in the demethyl esterification of seed mucilage by screening for PME mutants with defective extrusion or adherence. One such mutant, carrying a defect in the gene *At1g23200*, was shown to be required for normal embryo development. The defect in mucilage extrusion observed in the mutant was shown to be a pleiotropic effect of the changes in embryo.

RESULTS

Identification of *PME* Genes Expressed in the Seed Coat during Mucilage Secretion

Previously, we hypothesized that a *PME* gene involved in mucilage modification would be expressed between 4 and 9 DPA with a peak at approximately 7 DPA toward the end of the period of mucilage secretion (Haughn and Chaudhury, 2005). Using the eFP browser (http://bar.utoronto.ca/efp) and a seed coat-specific microarray (http://bar.utoronto.ca/efp_seedcoat/), we identified seven *PME*s expressed in the seed coat (Fig. 1). Two previous studies identified *AtPME*s with expression patterns specifically up-regulated in the silique (Louvet et al., 2006) and seed coat (Wolf et al., 2009). In these studies, the annotated genes *At5g49180*, *At1g11590*, *At4g03930*, and *At4g33220* were identified as being expressed in the seed in agreement with our results. We verified the in silico results for all seven genes using reverse transcription (RT)-PCR (Fig. 1).

The transcripts of two genes, *At1g23200* and *At2g43050*, were highest in the seed coat at 7 DPA (increased significantly from 4 to 7 DPA and decreased from 7 to 10 DPA) in the seed coat-specific microarray (http://bar.utoronto.ca/efp_seedcoat/). The expression of both genes is relatively low in other plant tissues, except the embryo (*At1g23200*) and stem (*At2g43050*; Fig. 1).

Insertion Lines with a Seed Mucilage Phenotype

We screened Arabidopsis insertional mutant lines available from the Arabidopsis Biological Resource Center, the Nottingham Arabidopsis Stock Center, and the RIKEN Bioresource Center for all seven annotated *PME* genes, except *At2g43050*. No insertions were confirmed in the transfer DNA (T-DNA) line ordered for *At2g43050*. Only one insertional mutant line (15-4955-1; transposon-tagged line from the RIKEN Genomic Sciences Center; Ito et al., 2002; Kuromori et al., 2004) gave an obvious mucilage phenotype. This line has an insert in the second exon of *At1g23200* (Fig. 2A), a gene encoding a PME, which we designated as *HIGHLY METHYL ESTERIFIED SEED* (*HMS*; the 15-4955-1 allele is *hms-1* in the Nossen-0 [Nos-0] background), because the mutant phenotype includes an increase in methyl esterification of seed tissue (see below). We verified that the expression of *At1g23200* in Nos-0 was similar to that observed for the Columbia-0 (Col-0) background (compare Fig. 1 with Supplemental Fig. S1). The *hms-1* mutant completely lacked *HMS* wild-type transcript (Fig. 2B), and when the *hms-1* mutant was exposed to water, mucilage extrusion was limited compared with the wild type (Fig. 2, E, F, K, and L). Analysis of an F2 population of 141 individuals from a cross between the wild type and the *hms-1* mutant showed a segregation pattern of 107 wild-type to 34 mutant plants, consistent with a single nuclear mutation ($\chi^2 = 0.167$, $P > 0.05$). Using PCR genotyping on the same population, the transposon insertion segregated 29:78:34 the wild type: heterozygote:homozygote (1:2:1; $\chi^2 = 0.548$, $P > 0.05$) and cosegregated with the seed phenotype consistent with the hypothesis that *hms-1* is caused by a transposon insertion. To further support the hypothesis that the phenotype is caused by a mutation in HMS, molecular complementation was performed. The *hms-1* mutant was transformed with a genomic DNA fragment (*HMS* promoter [*pHMS*]: *HMS*) spanning 1.9 kb upstream of the ATG start site to 0.3 kb downstream of the *HMS* stop codon. From 36 independent lines transformed, 24 showed complete rescue of the Arabidopsis transposon-tagged line phenotype, and transcript abundance was restored (Fig. 2, B, I, J, and N).

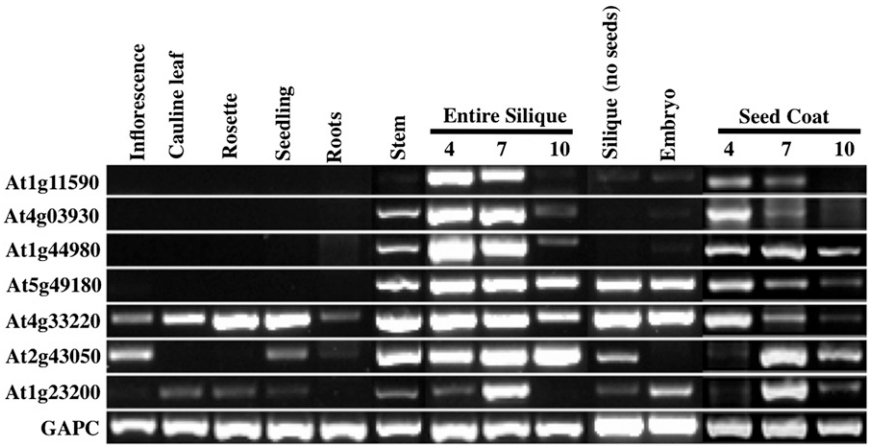

Figure 1. The expression of putative PME genes at different times and in various tissues of Arabidopsis. RT-PCR was used to identify the presence of transcripts from seven *PME* genes in different plant tissues. GAPC mRNA was used as an internal positive control.

We analyzed a second *hms* allele, allele gabi-kat-278G11 (renamed *hms-2*; www.gabi-kat.de). The T-DNA in *hms-2* is inserted at −29 from the +1 site in the 5′ untranslated region (UTR; Fig. 2A). The *hms-2* mutant has no mucilage phenotype, and HMS transcript in *hms-2* is comparable with the wild type. No other alleles were available in the coding region of *HMS*.

The Morphology of the *hms-1* Seed Coat and Embryo Is Affected

The mature *hms-1* seed morphology was altered compared with the wild type. The *hms-1* seeds appeared smaller in size and were irregular in shape (Fig. 2, C and D). When mature hydrated seeds were illuminated and observed by light microscopy, the *hms-1* seed appeared translucent, whereas the wild-type seeds were opaque. In addition, the mutant embryos appeared smaller and underdeveloped (Fig. 2, E and F), a conclusion supported by dissection of the embryos from the seed (Fig. 2, G and H). The total weight of the *hms-1* seeds was also found to be lower than that of the wild type (Fig. 2J).

The *hms-1* Mucilage Phenotype Is a Consequence of an Embryo Defect

Because the *hms-1* phenotype includes defects in both seed coat and embryo, we investigated whether the phenotype was caused by the genotype of the seed coat, the embryo, or both. The *hms-1* mutant was used as the female parent in a cross with the wild type. In this cross, the F1 seeds have a seed coat that is homozygous for *hms-1* and an embryo that is heterozygous for this mutation. The morphology, weight, and mucilage extrusion phenotypes of the F1 seeds were similar to those of the wild type (Fig. 2, K–M). Thus, the *hms-1* seed phenotype, including the characteristics for mucilage extrusion and the seed coat, is caused by loss of HMS function in the embryo but not the seed coat. Consequently, we investigated the embryo defects further.

The *hms-1* Embryo Defect Is First Visible at 7 DPA

To investigate the development of *hms-1* seeds, wild-type and *hms-1* seeds were sectioned at 4, 7, and 10 DPA. These times represent key stages in seed development. At 4 DPA, wild-type epidermal seed coat cells have finished growing but have not begun to synthesize mucilage (Fig. 3E). The wild-type embryo is at the heart stage (Fig. 3A), with large vacuolated cells (Fig. 3C). By 7 DPA, mucilage secretion in the seed coat epidermal cells is almost complete (Fig. 3K). The 7 DPA embryo has reached the bent cotyledon stage (Fig. 3G), and its cells are expanding and beginning to accumulate storage reserves (Fig. 3I). The seed coat epidermal cells of the 10-DPA seed have begun to synthesize a secondary cell wall (Fig. 3Q). Embryo morphogenesis and growth are almost complete (Fig. 3M), and its cells contain considerable storage reserves (Fig. 3O). The seed coat development of *hms-1* was similar to that of the wild type throughout development (compare Fig. 3, E, K, and Q with Fig. 3, F, L, and R). In contrast, the *hms-1* embryo was similar to the wild type around 4 DPA (Fig. 3, A and B) but different from the wild type by 7 DPA (Fig. 3, G and H). The *hms-1* embryo at 7 DPA was significantly smaller and appears to be at an earlier developmental stage (torpedo). These differences were more pronounced by 10 DPA (Fig. 3, M and N). The *hms-1* embryo defects (7 DPA) roughly coincide with *HMS* expression in wild-type seeds (Fig. 1).

The *hms-1* Embryo Cell Size Is Decreased

As shown above, the *hms-1* embryo is smaller relative to the wild-type embryo after 4 DPA (Fig. 3, G, H, M, and N). To determine the anatomical basis for this size change, the anatomies of wild-type and *hms-1* seeds at 4, 7, and 10 DPA were examined. Cells of the 4- and 7-DPA embryos were similar in structure to those of the wild type (Fig. 3, C, D, I, and J). However, at 10 DPA, *hms-1* embryo cells appeared smaller than the wild type, maintained their large vacuoles, and had fewer lipid bodies, a phenotype more closely resembling

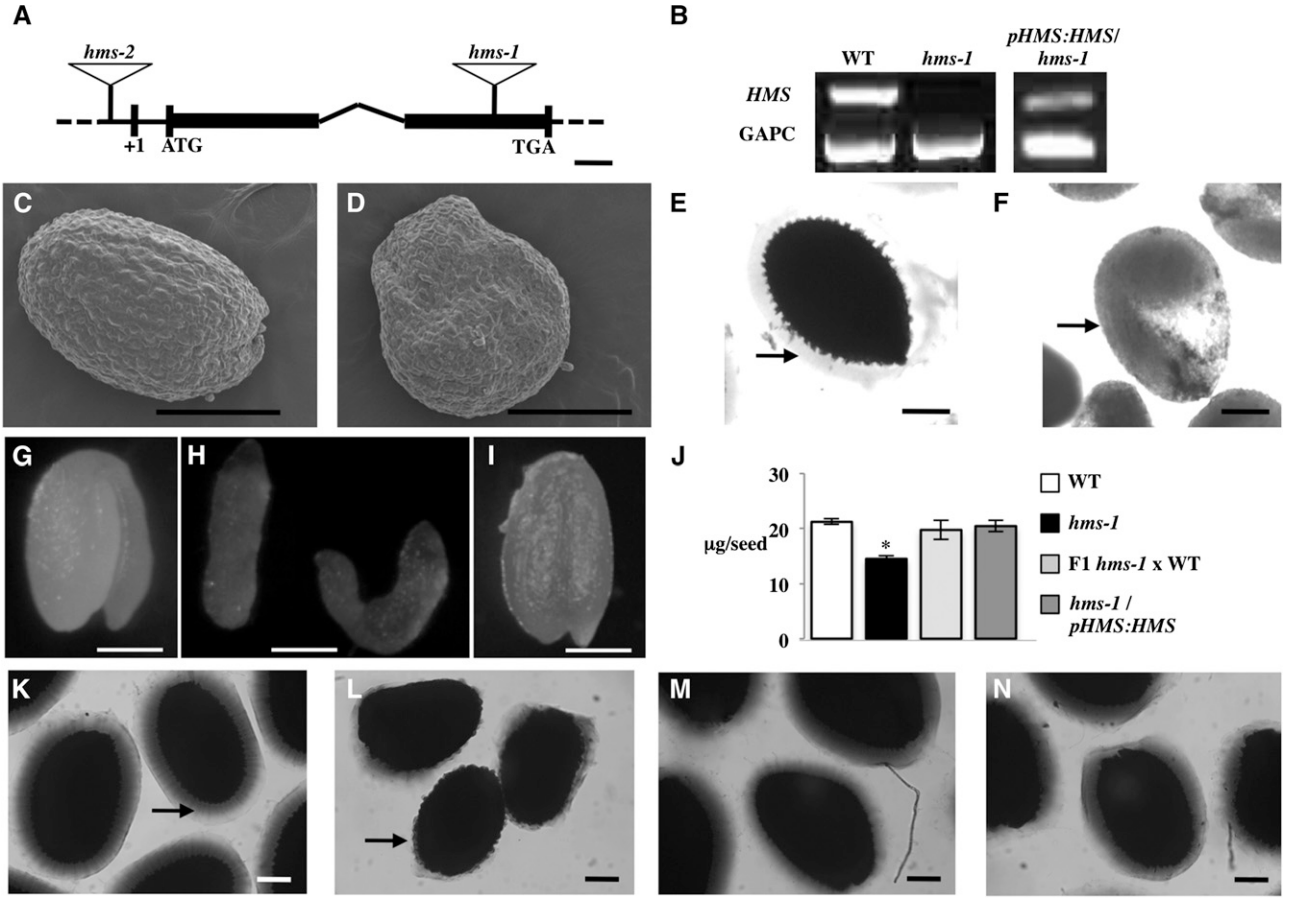

Figure 2. Seed phenotype of the *hms-1* mutant. A, *HMS* gene structure, including the position of the transposon insertion in *hms-1* and the T-DNA in *hms-2*. The two exons are represented by black boxes, and the intron is represented by the connecting line. B, *HMS* transcript accumulation in whole seeds at 7 DPA for wild-type, *hms-1*, and *pHMS*:*HMS*-transformed *hms-1* plants. RNA was extracted, and mRNA was detected by RT-PCR. GAPC mRNA was used as an internal control. C and D, Scanning electron microscope imaging. E and F, Seeds after shaking in water and subsequent staining with Ruthenium Red. The photographs of the wild type in E and *hms-1* in F were taken with illumination from below. G to I, Rehydrated embryos. J, Average seed weight in micrograms per seed. Values represent the mean ± SE of 30 replicates. *, Significant difference from the wild type using a Student's *t* test with a Bonferroni correction ($P < 0.05$). K to N, Mature seeds after shaking in water and subsequently staining in Ruthenium Red. Wild-type seeds are shown in C, E, G, and K; *hms-1* is shown in D, F, H, and L; *pHMS*:*HMS*-transformed *hms-1* seeds are shown in I and N; and F1 progeny are from the cross of *hms-1* and the wild type (M). Arrows point at mucilage for comparison between the wild type and *hms-1*. WT, Wild type. Bars = 100 μm.

the linear cotyledon stage of embryogenesis (Fig. 3, O and P). Measurement of the perimeter of the cells in sections was used as a means to quantify the cell sizes. Embryo cell sizes were similar between *hms-1* and the wild type at 4 to 7 DPA but significantly different at 10 DPA, when the *hms-1* radicals and cotyledons both had a reduced cell perimeter compared with the wild type (Fig. 3, S and T). These data suggest that cell expansion in the embryo is reduced in *hms-1*.

The Yellow Fluorescent Protein-HMS Protein Fusion Is Found in the Seed Coat and Embryo Cells

To investigate the localization of HMS, two constructs with Citrine Yellow Fluorescent Protein (YFP; Griesbeck et al., 2001) were generated: one with *YFP* fused in frame to the C terminus of *HMS* and one with the *YFP* positioned after the putative prepro domain ((PP; PP sequences function as signal peptides and/or play a crucial role in the folding of proproteins) of the HMS protein (HMS promoter [*pHMS*]:*HMS*::*YFP* and *pHMS*:*PP*::*YFP*::*HMS*). Of 64 *pHMS*:*HMS*::*YFP*- and 28 *pHMS*:*PP*::*YFP*::*HMS*-transformed lines, 9 and 6 lines, respectively, showed YFP fluorescence signal. None of the transformed lines carrying either construct showed complementation of the phenotype, suggesting that the HMS-YFP fusions did not have enough HMS activity to compensate for the *hms* mutation. However, both fusion constructs had similar temporal, spatial, and intracellular localization patterns for YFP in the seed (Fig. 4; Supplemental Fig. S2). Fluorescence was not observed

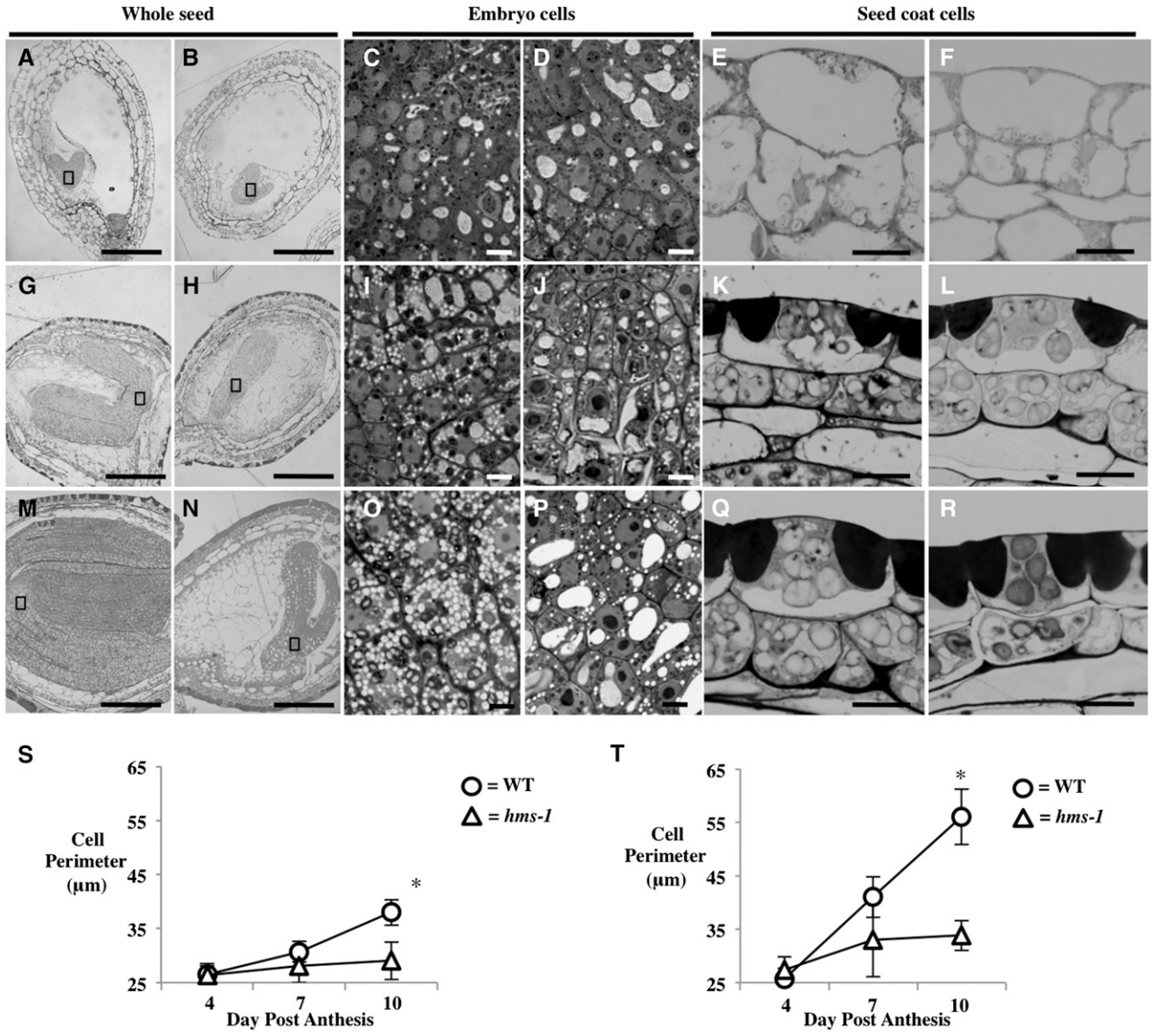

Figure 3. Seed anatomy and embryo cell sizes throughout development. Whole seeds, embryo cells, and seed coat cells section showing seeds at 4 DPA (A–F). G to L, Seeds at 7 DPA. M to R, Seeds at 10 DPA. Wild-type seeds are shown in A, C, E, G, I, K, M, O, and Q, and *hms-1* seeds are shown in B, D, F, H, J, L, N, P, and R. Bars in A, B, G, H, M, and N = 100 μm. Bars in C to F, I to L, and O to R = 6 μm. S and T, Average perimeter length of embryo cells. Cotyledon cells in S and radicule cells in T at 4, 7, and 10 DPA. Values represent the mean ± SE of 30 replicates. WT, Wild type. *, Significant difference using a Student's *t* test with a Bonferroni correction ($P < 0.05$).

in the *pHMS*:*HMS*::*YFP* and *pHMS*:*PP*::*YFP*::*HMS* plants at 4 DPA (Supplemental Fig. S2), whereas at 7 and 10 DPA, fluorescence was observed in the epidermal cell layer of the seed coat as well as multiple cell layers of the embryo (Fig. 4; Supplemental Fig. S2). The YFP signal in the epidermal cells of the seed coat colocalized with the cell wall stain propidium iodide that stained the primary cell wall (Fig. 4, A–C) and in the cell compartment outside the FM 4-64-stained plasma membrane (Fig. 4, D–F), supporting cell wall localization. In the embryo cells, the YFP signal partially colocalized with the cell wall marker propidium iodide, again suggesting cell wall location (Fig. 4, G–I). Examination of the merged YFP and FM 4-64 images of the embryo indicated that the YFP was present between the FM 4-64 signal of adjoining cells (Fig. 4L), again suggesting a partial cell wall localization. YFP fluorescence also colocalized with FM 4-64-stained circular structures within the cytoplasm, suggesting partial localization within the endomembrane system (Fig. 4, J–L). These results suggest that, as expected for a PME, HMS is targeted to the endomembrane system and secreted to the apoplast. However, in the absence of complementation, we cannot eliminate the possibility that the YFP tag results in mislocalization of HMS.

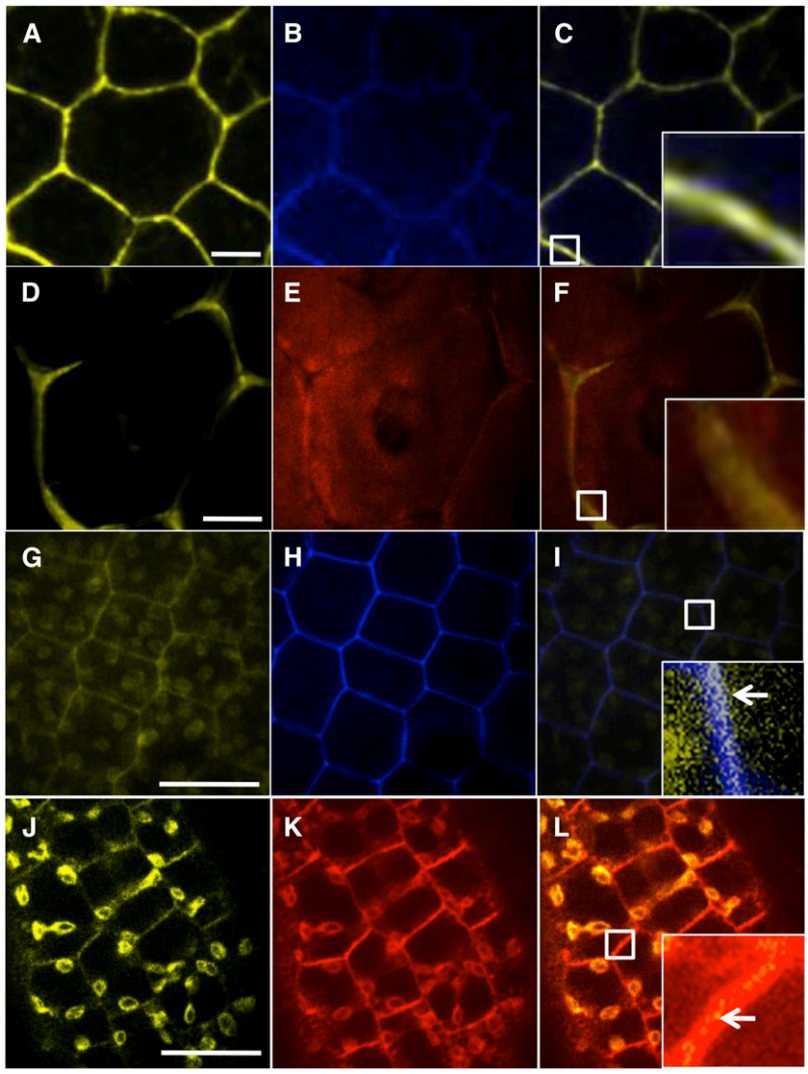

Figure 4. Localization of YFP-HMS in seed coat and embryo cells. A to F, Seven-DPA seed coat epidermal cells showing YFP signal in A and D, cell wall stained with propidium iodide in B, and membrane stain FM 4-64 in E as well as respective composite images in C and F. G to L, Seven-DPA embryo cells showing YFP signal in G and J, cell wall stain with propidium iodide in H, and membrane stain FM 4-64 in K, as well as respective composite images in I and L. To better indicate intracellular location of the YFP signal in the embryo cell, a section of the image composite is amplified (inset) in I and L. Bars = 10 μm.

The PME Activity Is Decreased and the Degree of Methyl Esterification Is Increased in *hms-1* 7-DPA Seeds

Expression in the yeast *Saccharomyces cerevisiae* of the HMS coding region both with and without the PME prodomain in the vector pESC-URA (Agilent Technologies) failed to show PME activity. As an alternative, measurements of the PME activity in protein extracts from developing 4-, 7-, and 10-DPA *hms-1* and wild-type seeds were used to test if the presence of HMS protein is correlated with PME activity. PME activity from 4-DPA developing siliques was similar in *hms-1* and the wild type (Fig. 5A). Unexpectedly, a significantly lower level of PME activity was observed in the F1 siliques of the *hms-1* and the wild-type cross at 4 DPA (Fig. 5A), a result that might have resulted from delayed or lowered fertilization as a consequence of outcrossing. By 7 DPA, PME activity was significantly lower in *hms-1* compared with the wild type (Fig. 5A). This activity in F1 seeds of the *hms-1* and the wild type cross was intermediate between the wild type and *hms-1*. Transformation with the *pHMS:HMS* construct was able to complement the loss of PME activity in *hms-1*. The 10-DPA seed protein extracts showed no PME activity in any sample (Fig. 5A). Because a decrease in PME is expected to result in an increase in the degree of methyl esterification (DM), the DM of the same extracts was quantified and showed a small but significant increase in the *hms-1* mutant only at 7 DPA (Fig. 5B). Interestingly, the difference in the DM was not conserved later in development. This suggests the need for a decrease in the DM specifically at 7 DPA for the embryo to develop properly.

The 7-DPA *hms-1* Embryos Have Increased Labeling by HG-Specific Antibodies

PME activity and DM of *hms-1* and *pHMS:HMS* leaves suggest that HMS is an active PME. Localizing pectin demethyl esterification in cross sections of seed can give additional information on the differences in DM between *hms-1* embryo and the wild type. To

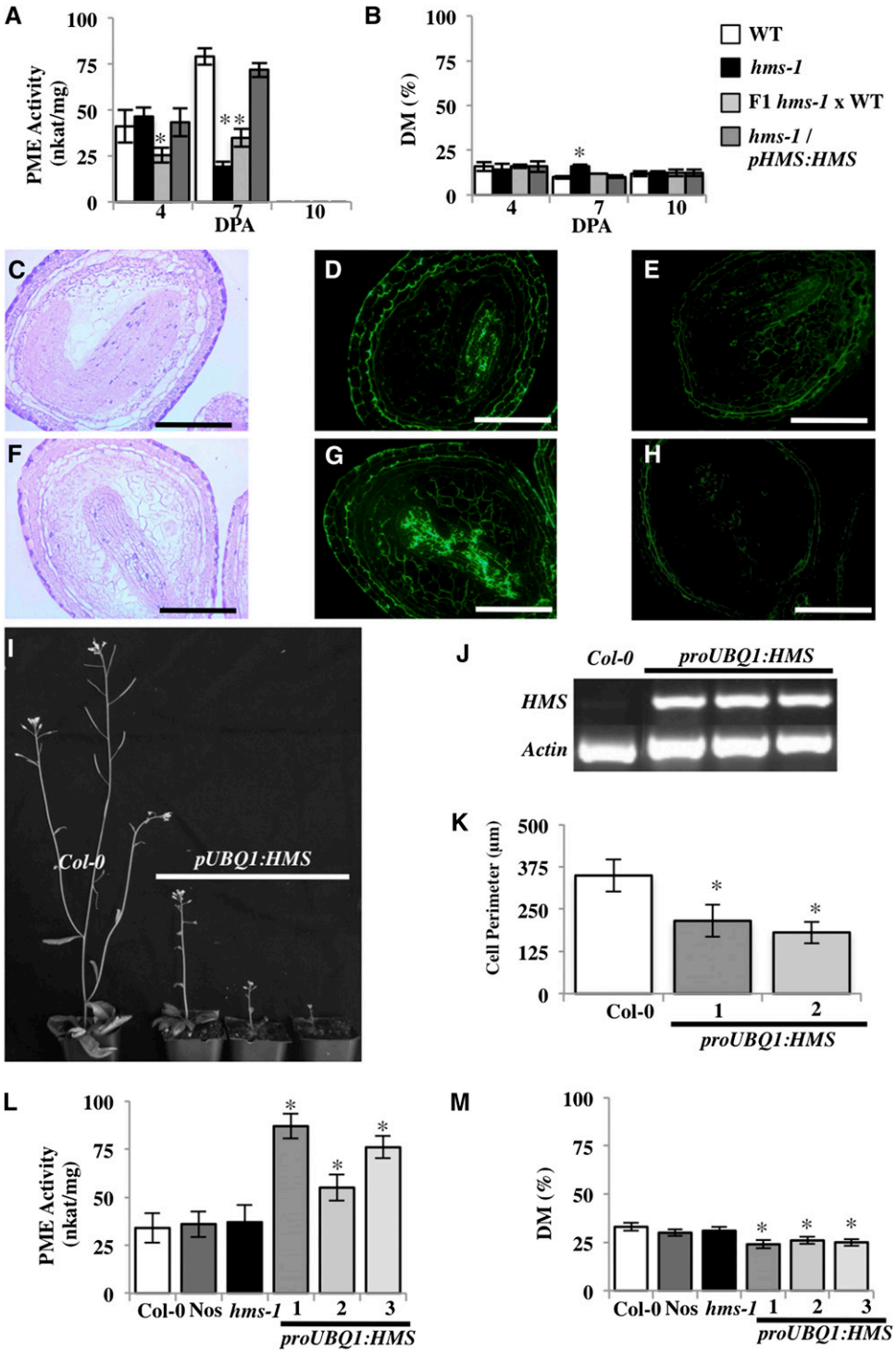

Figure 5. HMS influence on methyl esterification. A, PME activity in nanokatals per milligram of crude protein extracts from 4-, 7-, and 10-DPA developing seeds comparing the wild type, *hms-1*, F1 progeny from the cross *hms-1* and the wild type, and *pHMS*:*HMS*-transformed *hms-1* seeds. B, Biochemical determination of the percentage of methyl esters of galacturonic acid (GalUA) in developing seeds comparing the wild type, *hms-1*, F1 progeny from the cross *hms-1* and the wild type, and *pHMS*:*HMS*-transformed *hms-1* seeds. C to H, The binding of JIM5 and JIM7 antibodies to 7-DPA seed sections. Sections were stained with Toluene Blue in C and F, sections were immunolabeled with the antibody JIM7 in D and G, and sections were immunolabeled with the antibody JIM5 in E and H. The wild type is shown in C to E, and *hms-1* is shown in F to H. Bar = 100 μm. I, Twenty-six-day-old wild-type plants and three plants transformed with the *UBIQUITIN1 promoter* (*proUBQ1*):*HMS1*, *proUBQ1*:*HMS2*, and *proUBQ1*:*HMS3*. J, *HMS* transcript accumulation in wild-type and *proUBQ1*:*HMS*-transformed plants.

examine the DM of HG pectin in seeds, thin sections of developing seeds were treated with JIM7 and JIM5 antibodies, where the epitope for JIM7 is HG with a high DM and JIM5 is HG with a low DM (Willats et al., 2000, 2001). For the seed coat, no differences in the binding of either antibody were observed between *hms-1* and the wild type (Fig. 5; Supplemental Fig. S2). A similar result was found for JIM5 and JIM7 signals in the embryo at 4 DPA (Supplemental Fig. S3). However, by 7 DPA, JIM7 signal in the *hms-1* embryo seemed higher compared with the wild type. JIM7 binding is distributed through both the radical and cotyledon in the *hms-1* embryo, whereas in the wild type, it is restricted to the cotyledon (Fig. 5, D–G). In contrast, JIM5 appears slightly lower in 7-DPA *hms-1* compared with wild-type seed sections (Fig. 5, E–H). In 10-DPA *hms-1* and wild-type sections, the JIM7 binding is similarly distributed in the cotyledon and radical (Supplemental Fig. S3, H–K). JIM5 signal appears slightly lower in the *hms-1* embryo compared with the wild type (Supplemental Fig. S3, I–L). Taken together, the differences observed in the labeling of embryo by JIM5 and JIM7 are consistent with an increase in DM specific to the *hms-1* 7-DPA embryos.

Ectopic *HMS* Expression Causes Dwarfism and Increases the PME Activity

If the decrease in DM at 7 DPA is caused by a lack of HMS PME activity, expressing HMS ectopically may increase the PME activity and decrease the DM in tissues other than the seed. Lines expressing the *HMS* gene under the control of *proUBQ1* were generated. Of 14 transformed plants with the *proUBQ1*:*HMS* construct, five lines expressed *HMS* in the leaves where *HMS* is not normally expressed (Figs. 1 and 5J). Three independently transformed lines (*proUBQ1*:*HMS1*, *proUBQ1*:*HMS2*, and *proUBQ1*:*HMS3*) were studied. These plant lines were smaller than the wild type and seemed highly infertile (Fig. 5I). The PME activity in crude protein extracts isolated from *proUBQ1*:*HMS1*, *proUBQ1*:*HMS2*, and *proUBQ1*:*HMS3* leaves were higher relative to the wild type (Fig. 5L). The PME activity in *hms-1* leaves seemed the same as in the wild type, which is most likely because of the low level of HMS in this tissue in both the wild type and *hms-1*. This hypothesis is supported by the lack of YFP-tagged HMS signal seen in the leaves of transformants carrying *pHMS*:*PP*::*YFP*::*HMS* (data not shown). The DM in *proUBQ1*:*HMS1*, *proUBQ1*:*HMS2*, and *proUBQ1*:*HMS3* leaf extracts was decreased compared with the wild type (Fig. 5M), whereas the DM of *hms-1* leaf extracts was similar to the wild type (Fig. 5M). Because plants transformed with *proUBQ1*:*HMS* have a general decrease in plant size, the cell size in leaves was measured. The perimeter of leaf cells was significantly smaller in all plants tested compared with the wild type (Fig. 5K). This finding shows that HMS activity affects cell elongation.

PMEI5 Does Not Act through HMS in the Embryo Cell Wall

Ectopic expression of PMEI5 driven by the 35S promoter has been shown to produce larger seeds with a bigger embryo and faster germination rate (Müller et al., 2013). To verify if PMEI5 impacts HMS, we crossed a PMEI5 overexpression (OE) line with the *hms-1* mutant to generate an *hms-1*/PMEI5 OE line. The resultant *hms-1*/PMEI5 OE had seeds that looked similar to PMEI5 OE, with a bigger embryo and the same DM (Fig. 6). This suggests that PMEI5 does not act through HMS.

HMS Causes the Softening of Plant Tissues

PMEs can either strengthen or loosen the cell wall depending on the pattern of demethyl esterification. In an effort to assess the consequence of the lack of PME activity in *hms-1* on the rigidity of the tissue, we performed a dynamic mechanical analysis (DMA) by applying an increasing force between two clamps on equally distributed seed material and calculating the percentage of seed deformation. The resultant average seed deformation was reduced in the *hms-1* mutant compared with the wild type and the *hms-1* plants transformed with *pHMS*:*HMS* (Fig. 7). This result is consistent with the hypothesis that normal HMS activity promotes a loosening of seed cell wall tissue and that, in its absence, the tissues are more rigid and resistant to deformation. Although the change in seed deformation observed in this study may be a consequence of stiffer cell walls, we acknowledge that the size of the cells may be a major factor influencing the rigidity of the plant material and that the comparison between material of diverse size and morphology is not easily interpreted.

Figure 5. (*Continued.*)
RNA was extracted from leaves, and mRNA was detected by RT-PCR. Actin mRNA was used as an internal control. K, Average leaf epidermal cell perimeters comparing Col-0 wild-type with *proUBQ1*:*HMS1*- and *proUBQ1*:*HMS2*-transformed plants. Values represent the mean ± SE of 30 replicates. L, PME activity in nanokatals per milligram of crude protein extracts from leaves comparing wild-type Col-0 and Nos-0, *hms-1*, *proUBQ1*:*HMS1*, *proUBQ1*:*HMS2*, and *proUBQ1*:*HMS3*. M, Biochemical determination of the DM comparing wild-type Col-0 and Nos-0, *hms-1*, *proUBQ1*:*HMS1*, *proUBQ1*:*HMS2*, and *proUBQ1*:*HMS3*. Values represent the mean ± SE of four replicates in A, B, L, and M. WT, Wild type. *, Significant difference from the wild type using a Student's *t* test with a Bonferroni correction ($P < 0.05$) in A, B, K to M.

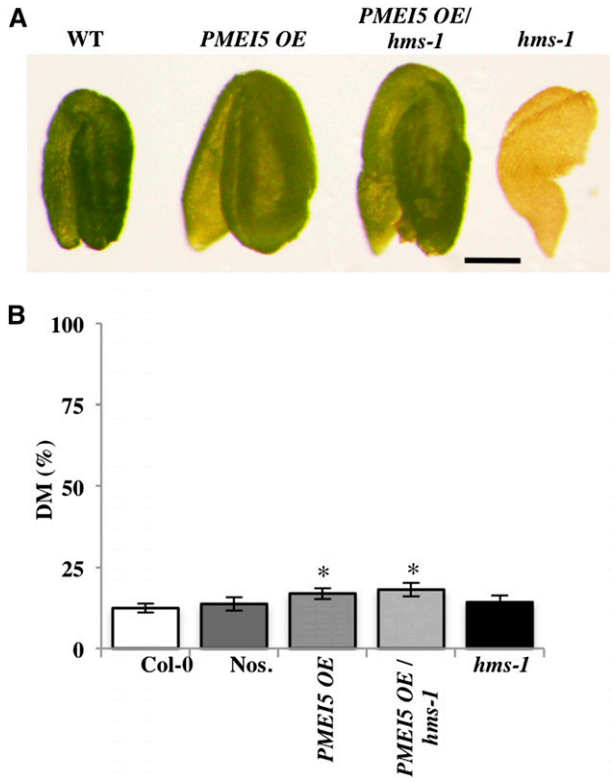

Figure 6. PMEI5 OE suppresses the *hms-1* mutant phenotype. A, Dissected mature embryos of the genotypes Col-0 PMEI5 OE, PMEI5 OE/*hms-1*, and *hms-1*. Bar = 100 μm. B, Biochemical determination of the percentage of methyl esters of GalUA in mature seed comparing the wild type, *hms-1*, PMEI5 OE, and F1 progeny from the cross between PMEI5 OE and *hms-1*. Values represent the mean ± SE of four replicates. WT, Wild type. *, Significant difference from the wild type using a Student's *t* test with a Bonferroni correction ($P < 0.05$).

DISCUSSION

HMS Encodes a PME

The annotation of HMS as a PME was assigned by sequence homology (the Arabidopsis Genome Initiative). Our research has generated several lines of evidence that support this annotation. First, there is a strong correlation between HMS function and PME activity in 7-DPA seed extracts. The loss of HMS function (in *hms-1*) resulted in a decrease in PME activity, whereas an increase in HMS expression (*proUBQ1:HMS*) caused an increase in PME activity (Fig. 5). These results show that HMS is needed for wild-type PME activity in seeds. Second, changes in HMS activity are correlated with the level of detectable DM in the seed (Fig. 5) and the binding of HG-specific antibodies that are sensitive to the DM (Fig. 5; Supplemental Fig. S2). Third, as expected for a PME (e.g. Morvan et al., 1998), the data support the idea that HMS is localized, at least partially, in the apoplast (Fig. 4). Therefore, our results support the hypothesis that HMS is an active PME.

HMS Plays an Important Role in Embryo Growth

HMS plays a profound role in embryo morphogenesis. After 4 DPA, *hms-1* embryos develop more slowly than the wild type, reaching, at most, the bent cotyledon stage (Figs. 2 and 3). The dry mature seed is wrinkled and weighs considerably less than the wild type. More specifically, the cells in the embryo are generally smaller in size and fail to accumulate the normal amount of storage compounds, including oil bodies (Fig. 3). Taken together, these results suggest that HMS functions to promote normal cell growth in the embryo. One important function of PMEs is to promote or inhibit cell wall expansion and elongation by stiffening (Moustacas et al., 1991; Al-Qsous et al., 2004; Liu et al., 2013) or loosening (Tieman et al., 1992; Pilling et al., 2004; Jiang et al., 2005; Francis et al., 2006) the cell wall. Because *HMS* encodes a PME, we suggest that HMS facilitates cell wall loosening at the stage when cell expansion is needed to complete morphogenesis and makes room for storage compound deposition (Fig. 3; see below). Our data, indicating that *hms-1* seeds are more resistant to deformation, and data of others, showing PME-induced changes in the DM impact the mechanical properties of the cell wall (Peaucelle et al., 2011), are consistent with this hypothesis.

Examples of Arabidopsis PME mutants causing developmental defects are limited (Jiang et al., 2005; Francis et al., 2006; Tian et al., 2006; Röckel et al., 2008; Guénin et al., 2011; Hongo et al., 2012). Furthermore, few plant PMEs have been associated with cell wall loosening, and physiological evidence for the involvement of PMEs in cell wall expansion is scarce (Moustacas

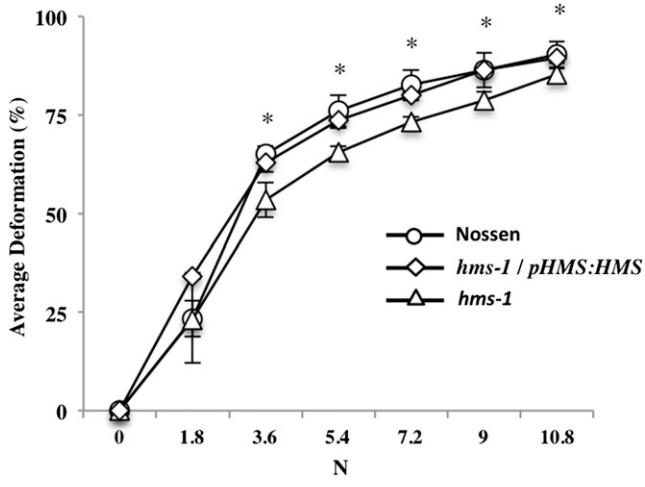

Figure 7. Seed deformation induced by increasing amounts of force. Average deformation in percentage of the total seed length comparing the wild type, *hms-1*, and *hms-1* transformed with the *pHMS:HMS* construct. Values represent the mean ± SE of 10 replicates. WT, Wild type. *, Significant difference using a Student's *t* test with a Bonferroni correction ($P < 0.05$).

et al., 1991; Al-Qsous et al., 2004; Peaucelle et al., 2011). The identification of *hms-1* with a seed embryo phenotype represents a unique function for PMEs in development. Our hypothesis for HMS function, outlined above, predicts that an increase in HMS activity in the embryo (e.g. *proUBQ1:HMS*) should enhance the loosening of the cell wall, producing a general increase in cell sizes. However, the ectopic expression of *HMS* in the plants transformed with *proUBQ1:HMS* resulted in smaller plants with smaller cells (Fig. 5). HMS protein may have a different function in other cell types or at other times in development because of distinct cell wall compositions and/or complement of cell wall-modifying proteins.

The Function of HMS in the Seed Coat Does Not Affect Mucilage Production

The initial goal of this investigation was to identify and characterize *PME* genes involved in seed mucilage modification to determine the effect of HG methylation on seed mucilage properties. Genes annotated as encoding PMEs expressed in the seed coat were identified, and insertion mutants for each gene were screened for mucilage phenotypes. *At1g23200* (*HMS*) was selected on the basis of its high seed coat expression at 7 DPA and the mucilage extrusion defects of the *hms-1* mutant. However, we have shown that the mucilage extrusion defects are a secondary effect of the loss of HMS function in the embryo. The *hms-1* seed coats have no obvious defects in differentiation or mucilage extrusion (Figs. 2 and 3) or the degree of HG methylation (Fig. 5; Supplemental Fig. S2). The strong expression of *HMS* in the seed coat suggests that HMS has a role in that tissue, but if so, its role is subtle, the phenotypic assays that we used were not sufficient, or the role is masked by redundancy. Because there are at least seven genes expressed in the seed coat, it is likely that one or more are redundant with HMS.

Cell Wall Loosening Enzymes Present in the Seed Other Than HMS May Act to Limit the Growth of the Embryo

OE PMEI5 plants have bigger seeds with bigger embryos (Müller et al., 2013), a phenotype contrasting with that of *hms-1*. Plants homozygous for *hms-1* having the OE PMEI5 construct have larger seeds, similar to those with OE PMEI5 alone (Fig. 6), indicating that PMEI5 function is not dependent on HMS. One possibility, consistent with this result, is that PMEI5 inhibits PMEs other than HMS, and this leads to a loosening of the cell wall in the seed, despite the absence of HMS activity. In roots, the OE of PMEI5 produced a root growth phenotype that required normal brassinosteroid signaling (Wolf et al., 2012, 2014). Thus, the exact mechanism by which PMEI5 suppresses the *hms* mutant phenotype is uncertain but could involve the activation of cell wall-modifying enzymes through brassinosteroid signaling.

CONCLUSION

The cell differentiation occurring during seed development involves complex cell wall modifications. PMEs influence cell wall rigidity and stiffening. HMS enzymatic activity is necessary for cell expansion and ultimately, growth. In addition, this study suggests an intricate interplay between HMS and other unidentified cell wall modifications involved in embryo cell expansion and development. The identification and characterization of additional cell wall-modifying enzymes acting on the embryo cell wall during development may help to determine the exact series of cell wall modifications that takes place during seed developments.

MATERIALS AND METHODS

Plant Material and Growth Conditions

Arabidopsis (*Arabidopsis thaliana*) plants of either Col-0 or Nos-0 genetic background were used in this study. Plants were grown as described by Dean et al. (2007), and flowers were staged as per the work by Western et al. (2000). Briefly, seeds were germinated on Arabidopsis medium plates (Haughn and Somerville, 1986) with 7% (w/v) agar, and seedlings were transferred to soil (Sunshine Mix; SunGro) after 7 d. Plants were grown in chambers with continuous fluorescent illumination (80–140 $\mu Em^{-2}\ s^{-1}$) at 20°C to 22°C. The Arabidopsis transposon-tagged line 15-4955-1 with an insert in the gene *At1g23200* was obtained from RIKEN Genomic Science Center (Ito et al., 2002; Kuromori et al., 2006).

PCR and Cloning

All DNA was amplified from Col-0 DNA using a two-step PCR protocol with long primers and Phusion High-Fidelity DNA Polymerase (New England Biolabs). The primers left primer (LP; CATTGCAAGGGTACCGGTCTATCACATTCATAACACACAATAAGCAAAA) and right primer (RP; CATTGCAAGCTCGAGAAGTCCATCGTTGACCGGTACTCCCGTAGCCGTAAT) were used to amplify the *pHMS:HMS*. The *pHMS:HMS* amplicon was introduced as a *Kpn*I-*Xho*I cassette into a pAD vector carrying Citrine YFP (DeBono, 2011). The *pHMS:HMS* amplicon starts 2,023 bp upstream of the ATG start site of HMS and ends just before the stop codon.

The *pCAMBIA2300* vector was modified by cloning the *Pst*I-*Xba*I 780-bp fragment carrying Citrine YFP, including spacers from pAD (DeBono, 2011), in the multicloning site to generate the construct pCAMBIA-YFPc. The primers LP (CATTGCAAGAAGCTTATTTCTTTCTCTTTTGAGTTTTAGTATCAAATATTTGTA) and RP (CATTGCAAGAAGCTTTTCCAGTAGTTTACGGTCGGAAAGAGGGAACCACGA) were used to amplify the *pHMS*, including the *PP*, resulting in a *pHMS:PP* amplicon. Each of these two primers includes an *Hin*dIII site that was used to clone the *pHMS:PP* fragment into the *Hin*dIII site of the pCAMBIA-YFPc vector upstream of and in frame with *Citrine YFP*. Also, an LP (cattgcaagTCTAGAGATTCCAAAACTACGGCAAAAGCCGATCTTGTGGTGG; nucleotides in lower case were added to increase efficiency of primer digestion with *Xpa*I), including an *Xba*I site, and an RP (CATTGCAAGGGTACCCAAAGCTACAATAAGAAAGGTAGAAAGATACATAA), including a *Kpn*I site, were used for the amplification of the remainder of the *HMS* coding region. This fragment was ligated into pCAMBIA-YFPc downstream of and in frame with the coding sequence of Citrine YFP to create *pHMS:PP::YFP::HMS*. The cloned *pHMS:PP* amplicon starts 2,372 bp upstream of the ATG of HMS and includes 723 bp of the coding region. The second *HMS* amplicon starts 723 bp downstream of the ATG start site of HMS and ends 300 bp downstream of the stop codon.

pGreenII 0029 was used to generate the construct pHMS:HMS. An LP (cattgcaagGGATCCacaaaaaacctcgaatcgatggaagacaaactccca) that included a *Bam*HI site and an RP (cattgcaagAAGCTTcaaagctacaataagaaaggtagaaagatacataa) that included an *Hin*dIII site were used to amplify *pHMS:HMS*. This *pHMS:HMS* amplicon starts 2,000 bp upstream of the ATG start site to 300 bp downstream of the stop codon and was inserted in *Bam*HI and *Hin*dIII sites in the pGreenII 0029 vector.

A modified *pCAMBIA2300* vector, including the *UBQ1* promoter, was a gift from Chris Ambrose (University of British Columbia) and used for the cloning of *UBQ1:HMS*. An LP (cattgcaagGGATCCaatatcccacatctctactcatccacattagtcaaaga) that included a *Bam*HI site and an RP (cattgcaagGGTACCaaatcttccaagagcgagtcaatcggtttgctattata) that include a *Kpn*I site were used to amplify the HMS genomic sequence, including both the 5′ and 3′ UTRs. The HMS amplicon starts 58 bp upstream of the 5′ UTR to 182 bp downstream of the 3′ UTR and was inserted into the *Bam*HI and *Kpn*I sites of the modified *pCAMBIA2300*.

RT-PCR Transcript Analysis

RNA was extracted from Col-0 and Nos-0 tissues using the PureLink RNA Mini Kit (Ambion) according to the manufacturer's instructions. RNA quantification was determined on a NanoDrop 8000 (Thermo Scientific). Five hundred nanograms of total RNA treated with DNase I (Invitrogen) was used for first-strand complementary DNA synthesis with SuperScript II Reverse Transcriptase (Invitrogen). RT-PCR was conducted using a typical PCR reaction containing Taq polymerase (Genescript) and gene-specific pairs of intron-spanning primers for *At1g23200*, *At1g11590*, *At4g03930*, *At1g44980*, *At5g49180*, *At4g33220*, *At2g43050*, and *Glyceraldehyde-3-Phosphate Dehydrogenase* (*GAPC*). Amplicons of approximately 200 bp were expected after intron splicing. Transcript levels were analyzed after 23 amplification cycles, and GAPC was used as a loading control.

Mucilage Extrusion and Staining

Whole mature seeds were hydrated and gently agitated in water for 45 min in a 1.5-mL microcentrifuge tube. Water was subsequently removed and replaced by 0.01% (w/v) Ruthenium Red (R2751; Sigma-Aldrich) for 30 min before a final wash in water. Hydrated seed samples were viewed using a light microscope. Bright-field micrographs of stained samples were taken with a digital camera (QImaging) equipped on a Zeiss AxioSkop 2 upright light microscope (Carl Zeiss; www.zeiss.com).

High-Pressure Freezing, Freeze Substitution, and Immunolabeling

Developing seeds at 4, 7, and 10 DPA were high-pressure frozen, resin embedded, and sectioned according to a previously published method (Rensing et al., 2002; Young et al., 2008). Developing seeds at 4, 7, and 10 DPA were dissected and pierced with an insect pin before being frozen in the presence of hexadecene using a Leica EM HPM 100 High-Pressure Freezer (Leica). Arabidopsis Nos-0 was used as the wild type. Freeze substitution base with 8% (v/v) dimethoxypropane in acetone, including 2% (w/v) osmium tetroxide as a general stain, and 0.25% (v/v) glutaraldehyde with 2% (w/v) uranyl acetate was used for immunolabeling assays. Freeze substitution was performed at −80°C using acetone with an increasing amount of resin. The samples were slowly infiltrated with Spurr's (Spurr, 1969) resin for morphological assays and LR white (London Resin Company; www.2spi.com) for immunological studies. Thin sections (0.5 μm) were used for both staining and immunolabeling. Sections were transferred and dried on Hydrophobic Printed Well Slides ER202W (Thermo Scientific). Slides were blotted in the presence of JIM5 and JIM7 antibodies in specific buffer as previously described (www.plantprobes.net).

PME Activity

PME activity was assayed using a modified version of a previously published method (Grsic-Rausch and Rausch, 2004). Briefly, approximately 1 mg of developing seeds was dissected from the silique and immediately frozen with liquid nitrogen. After grinding in liquid nitrogen, 100 μL of protein extraction buffer (100 mM Tris-HCL, pH 7.5, 500 mM NaCl, and cOmplete, Mini, EDTA-Free [Roche]) was added to the samples. The samples were mixed for 15 min at 4°C before centrifugation at 10,000*g* for 5 min at 4°C; 10 μL of supernatant was added to 100 μL (2 units of formaldehyde dehydrogenase in the presence of 5% [w/v] 80% Methyl-Esterified Pectin [P9135; Sigma-Aldrich] in a 0.4 mM NAD and 50 mM phosphate buffer, pH 7.5) using a 96-well plate assay read with a Synergy HT plate reader (BioTek). The protein concentration for each sample was measured using Protein Assay Kit I 500-0001 (Bio-Rad) with a standard curve made of Albumin Standard 23209 (Pierce).

Biochemical Determination of the DM

The methyl ester content was determined using a modified version of the protocol described by Lionetti et al. (2007). Approximately 5 mg of developing seeds was frozen in liquid nitrogen and ground to a fine powder. The ground seeds were washed two times with 70% (v/v) ethanol, one time with methanol: chloroform (1:1), and three times with acetone. Samples were dried under nitrogen gas at 60°C between each wash. After the final drying, samples were saponified in 0.25 M NaOH for 60 min and neutralized with 0.25 M HCl. Fifty microliters of supernatant was then loaded into a 96-well plate for methanol assessment (Lionetti et al., 2007).

The GalUA content was determined using a previously described protocol (van den Hoogen et al., 1998; Voiniciuc et al., 2013), where whole-seed carbohydrates remaining after saponification were precipitated in 100% ethanol by centrifugation. The pellets were dried under nitrogen gas at 60°C before being resuspended in distilled water. Samples were sonicated for 20 s with a Branson Sonifier 150 (Branson Ultrasonics; www.emersonindustrial.com) to create a homogenous suspension. Twenty microliters of each sample was used for the 96-well plate uronic acid assay (van den Hoogen et al., 1998).

Scanning Electron Microscopy

Dried Arabidopsis seeds were mounted on stubs and coated with gold-palladium alloy using the Hummer VI sputtering system (Anatech; anatech.com). The samples were then observed with a Hitachi S-800 scanning electron microscope, and images were captured with an Evex Nano Analysis digital imaging system (www.evex.com).

Confocal Microscopy

Developing *pHMS:pp:YFP::HMS* and wild-type seeds were mounted with water between a glass slide and a coverslip. Images were captured in darkness immediately after being exposed to propidium iodide (Sigma-Aldrich) or FM 4-64 (Invitrogen) for 5 and 10 min, respectively. Imaging was performed on an Olympus FV1000 laser-scanning confocal microscope using a 63× numerical aperture oil immersion objective. All image processing was performed using Olympus Fluoview software (www.olympusamerica.com) and Velocity (PerkinElmer, Inc.). All confocal micrographs were processed and assessed using ImageJ (Albramoff et al., 2004).

DMA

For mechanical tests, five mature seeds were placed between two specimen discs 15 mm in diameter (Electron Microscopy Sciences; www.emsdiasum.com). The position of seed samples was similar for each analysis. The samples were mounted on a QSeries Q800-0174 DMA (TA Instruments) and held in controlled force mode with the clamp compression applying a ramp force of 18 N min^{-1} to the specimens at room temperature. Specific deformations were recorded at 0, 1.8, 3.6, 5.4, 7.2, 9, and 10.8 N force before the plateau was reached. The percentage of total seed deformation was calculated using the position measured by the clamp.

Supplemental Data

The following supplemental materials are available.

Supplemental Figure S1. HMS expression.

Supplemental Figure S2. YFP:HMS and HMS:YFP expression.

Supplemental Figure S3. Four- to 10-DPA immunolabeled sections.

ACKNOWLEDGMENTS

We thank Dr. Chris Ambrose (University of British Columbia) for providing the modified *pCAMBIA2300* vector, including the *UBQ1* promoter, Dr. Allan Debono (University of British Columbia) for providing the *pAD* binary vector, Kevin Hodgson and Garnet Martens (University of British Columbia Bioimaging Facility) for assistance with microscopy, and Dr. Erin Gilchrist (University of British Columbia) for comments and critical reading of the article.

Received December 14, 2014; accepted January 6, 2015; published January 8, 2015.

LITERATURE CITED

Albramoff MD, Magalhaes PJ, Ram SJ (2004) Image processing with ImageJ. Biophonetics Int **11:** 36–42

Al-Qsous S, Carpentier E, Klein-Eude D, Burel C, Mareck A, Dauchel H, Gomord V, Balangé AP (2004) Identification and isolation of a pectin methylesterase isoform that could be involved in flax cell wall stiffening. Planta **219:** 369–378

Caffall KH, Mohnen D (2009) The structure, function, and biosynthesis of plant cell wall pectic polysaccharides. Carbohydr Res **344:** 1879–1900

Caffall KH, Pattathil S, Phillips SE, Hahn MG, Mohnen D (2009) *Arabidopsis thaliana* T-DNA mutants implicate *GAUT* genes in the biosynthesis of pectin and xylan in cell walls and seed testa. Mol Plant **2:** 1000–1014

Dean GH, Zheng H, Tewari J, Huang J, Young DS, Hwang YT, Western TL, Carpita NC, McCann MC, Mansfield SD, et al (2007) The *Arabidopsis MUM2* gene encodes a beta-galactosidase required for the production of seed coat mucilage with correct hydration properties. Plant Cell **19:** 4007–4021

DeBono AG (2011) The role and behavior of Arabidopsis thaliana lipid transfer proteins during cuticular wax deposition. PhD thesis. University of British Columbia, Vancouver, British Columbia, Canada

Francis KE, Lam SY, Copenhaver GP (2006) Separation of Arabidopsis pollen tetrads is regulated by *QUARTET1*, a pectin methylesterase gene. Plant Physiol **142:** 1004–1013

Goldberg R, Morvan C, Jauneau A, Jarvis MC (1996) Methyl-esterification, de-esterification and gellation of pectins in the primary cell wall. *In* J Visser, AGT Voragen, eds, Pectins and Pectinases. Elsevier, Amsterdam, pp 151–171

Griesbeck O, Baird GS, Campbell RE, Zacharias DA, Tsien RY (2001) Reducing the environmental sensitivity of yellow fluorescent protein. Mechanism and applications. J Biol Chem **276:** 29188–29194

Grsic-Rausch S, Rausch T (2004) A coupled spectrophotometric enzyme assay for the determination of pectin methylesterase activity and its inhibition by proteinaceous inhibitors. Anal Biochem **333:** 14–18

Guénin S, Mareck A, Rayon C, Lamour R, Assoumou Ndong Y, Domon JM, Sénéchal F, Fournet F, Jamet E, Canut H, et al (2011) Identification of pectin methylesterase 3 as a basic pectin methylesterase isoform involved in adventitious rooting in *Arabidopsis thaliana*. New Phytol **192:** 114–126

Haughn G, Chaudhury A (2005) Genetic analysis of seed coat development in Arabidopsis. Trends Plant Sci **10:** 472–477

Haughn GW, Somerville CR (1986) Sulfonylurea-resistant mutants of *Arabidopsis thaliana*. Mol Gen Genet **204:** 430–434

Haughn GW, Western TL (2012) *Arabidopsis* seed coat mucilage is a specialized cell wall that can be used as a model for genetic analysis of plant cell wall structure and function. Front Plant Sci **3:** 64

Hongo S, Sato K, Yokoyama R, Nishitani K (2012) Demethylesterification of the primary wall by PECTIN METHYLESTERASE35 provides mechanical support to the *Arabidopsis* stem. Plant Cell **24:** 2624–2634

Ito T, Motohashi R, Kuromori T, Mizukado S, Sakurai T, Kanahara H, Seki M, Shinozaki K (2002) A new resource of locally transposed *Dissociation* elements for screening gene-knockout lines in silico on the Arabidopsis genome. Plant Physiol **129:** 1695–1699

Jiang L, Yang SL, Xie LF, Puah CS, Zhang XQ, Yang WC, Sundaresan V, Ye D (2005) *VANGUARD1* encodes a pectin methylesterase that enhances pollen tube growth in the *Arabidopsis* style and transmitting tract. Plant Cell **17:** 584–596

Jolie RP, Duvetter T, Van Loey AM, Hendrickx ME (2010) Pectin methylesterase and its proteinaceous inhibitor: a review. Carbohydr Res **345:** 2583–2595

Kuromori T, Hirayama T, Kiyosue Y, Takabe H, Mizukado S, Sakurai T, Akiyama K, Kamiya A, Ito T, Shinozaki K (2004) A collection of 11 800 single-copy Ds transposon insertion lines in *Arabidopsis*. Plant J **37:** 897–905

Kuromori T, Wada T, Kamiya A, Yuguchi M, Yokouchi T, Imura Y, Takabe H, Sakurai T, Akiyama K, Hirayama T, et al (2006) A trial of phenome analysis using 4000 Ds-insertional mutants in gene-coding regions of *Arabidopsis*. Plant J **47:** 640–651

Lionetti V, Raiola A, Camardella L, Giovane A, Obel N, Pauly M, Favaron F, Cervone F, Bellincampi D (2007) Overexpression of pectin methylesterase inhibitors in Arabidopsis restricts fungal infection by *Botrytis cinerea*. Plant Physiol **143:** 1871–1880

Liu Q, Talbot M, Llewellyn DJ (2013) Pectin methylesterase and pectin remodelling differ in the fibre walls of two gossypium species with very different fibre properties. PLoS ONE **8:** e65131

Louvet R, Cavel E, Gutierrez L, Guénin S, Roger D, Gillet F, Guerineau F, Pelloux J (2006) Comprehensive expression profiling of the pectin methylesterase gene family during silique development in *Arabidopsis thaliana*. Planta **224:** 782–791

Macquet A, Ralet MC, Kronenberger J, Marion-Poll A, North HM (2007) *In situ*, chemical and macromolecular study of the composition of Arabidopsis thaliana seed coat mucilage. Plant Cell Physiol **48:** 984–999

Micheli F (2001) Pectin methylesterases: cell wall enzymes with important roles in plant physiology. Trends Plant Sci **6:** 414–419

Morvan O, Quentin M, Jauneau A, Mareck A, Morvan C (1998) Immunogold localization of pectin methylesterases in the cortical tissues of flax hypocotyl. Protoplasma **202:** 175–184

Moustacas AM, Nari J, Borel M, Noat G, Ricard J (1991) Pectin methylesterase, metal ions and plant cell-wall extension. The role of metal ions in plant cell-wall extension. Biochem J **279:** 351–354

Müller K, Levesque-Tremblay G, Bartels S, Weitbrecht K, Wormit A, Usadel B, Haughn G, Kermode AR (2013) Demethylesterification of cell wall pectins in Arabidopsis plays a role in seed germination. Plant Physiol **161:** 305–316

North HM, Berger A, Saez-Aguayo S, Ralet MC (2014) Understanding polysaccharide production and properties using seed coat mutants: future perspectives for the exploitation of natural variants. Ann Bot **114:** 1251–1263

Peaucelle A, Louvet R, Johansen JN, Höfte H, Laufs P, Pelloux J, Mouille G (2008) *Arabidopsis* phyllotaxis is controlled by the methyl-esterification status of cell-wall pectins. Curr Biol **18:** 1943–1948

Peaucelle A, Louvet R, Johansen JN, Salsac F, Morin H, Fournet F, Belcram K, Gillet F, Höfte H, Laufs P, et al (2011) The transcription factor BELLRINGER modulates phyllotaxis by regulating the expression of a pectin methylesterase in *Arabidopsis*. Development **138:** 4733–4741

Pelletier S, Van Orden J, Wolf S, Vissenberg K, Delacourt J, Ndong YA, Pelloux J, Bischoff V, Urbain A, Mouille G, et al (2010) A role for pectin de-methylesterification in a developmentally regulated growth acceleration in dark-grown *Arabidopsis* hypocotyls. New Phytol **188:** 726–739

Pelloux J, Rustérucci C, Mellerowicz EJ (2007) New insights into pectin methylesterase structure and function. Trends Plant Sci **12:** 267–277

Pilling J, Willmitzer L, Bücking H, Fisahn J (2004) Inhibition of a ubiquitously expressed pectin methyl esterase in *Solanum tuberosum L.* affects plant growth, leaf growth polarity, and ion partitioning. Planta **219:** 32–40

Rautengarten C, Usadel B, Neumetzler L, Hartmann J, Büssis D, Altmann T (2008) A subtilisin-like serine protease essential for mucilage release from *Arabidopsis* seed coats. Plant J **54:** 466–480

Rensing KH, Samuels AL, Savidge RA (2002) Ultrastructure of vascular cambial cell cytokinesis in pine seedlings preserved by cryofixation and substitution. Protoplasma **220:** 39–49

Ridley BL, O'Neill MA, Mohnen D (2001) Pectins: structure, biosynthesis, and oligogalacturonide-related signaling. Phytochemistry **57:** 929–967

Röckel N, Wolf S, Kost B, Rausch T, Greiner S (2008) Elaborate spatial patterning of cell-wall PME and PMEI at the pollen tube tip involves PMEI endocytosis, and reflects the distribution of esterified and de-esterified pectins. Plant J **53:** 133–143

Saez-Aguayo S, Ralet MC, Berger A, Botran L, Ropartz D, Marion-Poll A, North HM (2013) PECTIN METHYLESTERASE INHIBITOR6 promotes *Arabidopsis* mucilage release by limiting methylesterification of homogalacturonan in seed coat epidermal cells. Plant Cell **25:** 308–323

Spurr AR (1969) A low-viscosity epoxy resin embedding medium for electron microscopy. J Ultrastruct Res **26:** 31–43

Staehelin LA, Moore I (1995) The plant Golgi apparatus: structure, functional organization and trafficking mechanisms. Annu Rev Plant Physiol Plant Mol Biol **46:** 261–288

Sterling JD, Quigley HF, Orellana A, Mohnen D (2001) The catalytic site of the pectin biosynthetic enzyme alpha-1,4-galacturonosyltransferase is located in the lumen of the Golgi. Plant Physiol **127:** 360–371

Tan L, Eberhard S, Pattathil S, Warder C, Glushka J, Yuan C, Hao Z, Zhu X, Avci U, Miller JS, et al (2013) An *Arabidopsis* cell wall proteoglycan consists of pectin and arabinoxylan covalently linked to an arabinogalactan protein. Plant Cell **25:** 270–287

Tian GW, Chen MH, Zaltsman A, Citovsky V (2006) Pollen-specific pectin methylesterase involved in pollen tube growth. Dev Biol **294:** 83–91

Tieman DM, Harriman RW, Ramamohan G, Handa AK (1992) An antisense pectin methylesterase gene alters pectin chemistry and soluble solids in tomato fruit. Plant Cell **4:** 667–679

van den Hoogen BM, van Weeren PR, Lopes-Cardozo M, van Golde LM, Barneveld A, van de Lest CH (1998) A microtiter plate assay for the determination of uronic acids. Anal Biochem **257:** 107–111

Voiniciuc C, Dean GH, Griffiths JS, Kirchsteiger K, Hwang YT, Gillett A, Dow G, Western TL, Estelle M, Haughn GW (2013) Flying saucer1 is a transmembrane RING E3 ubiquitin ligase that regulates the degree of pectin methylesterification in *Arabidopsis* seed mucilage. Plant Cell **25:** 944–959

Wakabayashi K, Hoson T, Huber DJ (2003) Methyl de-esterification as a major factor regulating the extent of pectin depolymerization during fruit ripening: a comparison of the action of avocado (*Persea americana*) and tomato (*Lycopersicon esculentum*) polygalacturonases. J Plant Physiol **160:** 667–673

Wang M, Yuan D, Gao W, Li Y, Tan J, Zhang X (2013) A comparative genome analysis of PME and PMEI families reveals the evolution of pectin metabolism in plant cell walls. PLoS ONE **8:** e72082

Western TL, Skinner DJ, Haughn GW (2000) Differentiation of mucilage secretory cells of the Arabidopsis seed coat. Plant Physiol **122:** 345–356

Willats WG, Limberg G, Buchholt HC, van Alebeek GJ, Benen J, Christensen TMIE, Visser J, Voragen A, Mikkelsen JD, Knox JP (2000) Analysis of pectic epitopes recognised by hybridoma and phage display monoclonal antibodies using defined oligosaccharides, polysaccharides, and enzymatic degradation. Carbohydr Res **327:** 309–320

Willats WG, McCartney L, Knox JP (2001) *In-situ* analysis of pectic polysaccharides in seed mucilage and at the root surface of *Arabidopsis thaliana*. Planta **213:** 37–44

Wolf S, Mouille G, Pelloux J (2009) Homogalacturonan methyl-esterification and plant development. Mol Plant **2:** 851–860

Wolf S, Mravec J, Greiner S, Mouille G, Höfte H (2012) Plant cell wall homeostasis is mediated by brassinosteroid feedback signaling. Curr Biol **22:** 1732–1737

Wolf S, van der Does D, Ladwig F, Sticht C, Kolbeck A, Schürholz AK, Augustin S, Keinath N, Rausch T, Greiner S, et al (2014) A receptor-like protein mediates the response to pectin modification by activating brassinosteroid signaling. Proc Natl Acad Sci USA **111:** 15261–15266

Young RE, McFarlane HE, Hahn MG, Western TL, Haughn GW, Samuels AL (2008) Analysis of the Golgi apparatus in *Arabidopsis* seed coat cells during polarized secretion of pectin-rich mucilage. Plant Cell **20:** 1623–1638

Zhang GF, Staehelin LA (1992) Functional compartmentation of the Golgi apparatus of plant cells: immunocytochemical analysis of high-pressure frozen- and freeze-substituted sycamore maple suspension culture cells. Plant Physiol **99:** 1070–1083